

# Laser Fiber and Flexible Ureterorenoscopy: The “Safety Distance” Concept

M. Talso<sup>1,3</sup>, E. Emiliani<sup>1,4</sup>, M. Haddad<sup>1,2</sup>, L. Berthe<sup>2</sup>, M. Baghdadi<sup>1</sup>, E. Montanari<sup>3</sup>, O. Traxer<sup>1</sup>

<sup>1</sup>Department of Urology, Hôpital Tenon, Université Pierre et Marie Curie – Paris VI 4 rue de la Chine, 75020 Paris, France

<sup>2</sup>Laboratoire PIMM – UMR 8006 Ecole Nationale des Arts et Métiers – 131 Boulevard de l’Hôpital, 75013 Paris, France

<sup>3</sup>Departemnt of Urology, Fondazione IRCCS Ca’Granda Ospedale Maggiore Policlinico, Università degli Studi di Milano, Via Commenda 15 20122 Milano, Italy

<sup>4</sup>Universitat Autònoma de Barcelona

**Running title:** Ho-YAG laser cavitation bubbles and fURS damages

## Introduction

Flexible ureterorenoscopy is often used in the treatment of kidney stones and upper urinary tract transitional cell carcinoma. Because of the high cost of flexible ureterorenoscopes (fURSs) and their repair, extensive knowledge of the proper handling of the instruments is needed. Knowledge about the scopes, fibers, and laser settings is important for obtaining the best results, ensuring patient safety, and avoiding damage to the instruments. Many studies have shown that the longevity of a fURS depends on the experience of the surgeon and operating room team, the sterilization process used, and the type of procedures performed.<sup>1,2</sup> There is a wide range in the rate of damage of fURSs and repair costs.<sup>3–5</sup> There are insufficient data about the proper distance between the laser fiber’s tip and the scope to avoid instrumental damage caused by cavitation bubbles. We performed an observational study to evaluate the best position for the laser fiber to avoid fURS tip damage. In this study, we used different laser settings and positioned the laser fiber at different distances from the tip of the scope.

## Material and Methods

An in vitro observational study was performed. Seven fURS were tested including both fiber-optic (OU) and digital (DU) fURSs: Olympus P6 (OU), Olympus V (DU), Olympus V2 (DU), Wolf Boa (DU), Wolf Cobra Vision (DU), Storz XC (DU), and Boston Scientific LithoVue (DU). Initially, the laser fiber was loaded into the working channel of the different fURSs. A 273- $\mu$ m laser fiber and a 30 W Holmium laser YAG (Ho:YAG) machine (Rocamed) were used. The distance from the laser fiber tip and the fURS camera was measured with a ruler by a single investigator at the first appearance on the endoscopic screen (D1) and when the fiber reached one-quarter of the screen width (D2) (Table 1 and Fig. 1).

To evaluate the effect of Ho:YAG bubbles at different fiber distances, we assessed the size and shape of the bubble created at the tip of the fiber when the laser was activated. Videos were taken of four different scenarios in saline solution: with no working material, with a sample of pork kidney as soft tissue, with a synthetic hard stone simulating a calcium oxalate monohydrate calculus, and with a synthetic soft stone simulating an acid uric stone. The stone phantoms were prepared using BegoStone powder according to the indications of Esch et al.<sup>6</sup> Images of the laser activation were recorded at the tip of the fiber using a Photron APX-RS 3000 high-speed camera with a setting of 30,000 frames per second (fps) when the fiber was 1 and 2 mm outside the scope and at 15,000 fps when the fiber was a 3 mm outside the scope. The different fps settings were needed because when the fiber was at 3 mm, the camera's field of view was not wide enough to capture the entire image with a 30,000 fps capture setting.

The evaluations were performed with the laser fiber tip at 1, 2, and 3 mm from the fURS camera. Before the laser activation, two investigators checked the distance of the laser fiber from the scope at 1, 2, and 3 mm with a ruler. The fURS was fixed on a robot arm, and the position of the scope related to the target position was fixed and maintained by the robot (Fig. 2, img. 1). Different laser settings were used to provide a variety of output energy conditions

to simulate the dusting and fragmentation of the different kinds of stones and the ablation of pork kidney tissue by using both short and long pulse combinations (Table 2).

Finally, with the laser fiber at 3 mm, three combinations of joules (J) and hertz (Hz) (0.5 J, 10 Hz; 1 J, 10 Hz; 2 J, 5 Hz) were tested with no working material and with the synthetic soft stone. These were changed for each setting of pulse length to check for differences in the bubble dimensions between short and long pulses. The two major diameters of the bubbles were measured using ImageJ software. The distance between the stone and the fiber tip was 1 mm. We performed all experiments with the tip of the laser fiber cut to eliminate the distal transparent part. For the laser test, we used the fURS LithoVue system from Boston Scientific.

## Results

The first appearance on the screen of the laser tip differed between different scopes. Both the Wolf Cobra Vision and the Wolf Boa had the same D1, which was 1 mm and was the shortest of all scopes tested. The Storz XC had the longest distance at D2: 4 mm. For all scopes, D1 was 1–2 mm and D2 was 3–4 mm. Our recording of the bubble generated by the laser showed that at the 1 mm distance, regardless of the laser setting and the kind of tissue in front of the scope, the energy rebounded on the scope's tip (Fig. 3). The only situation in which the bubble did not return to the scope surface at the 1 mm distance occurred when the laser was activated in 0.9% NaCl solution without anything in front and at low energy (0.5 J) and long pulse duration (Fig. 4). At the 2 mm distance, using different machine settings and different scenarios, we never observed the bubble touching the fURS tip. At the same distance, we observed some stone dust rebound on the fURS camera when the laser was activated with energy >1 J regardless of the length of the pulses. At the 3 mm distance, the bubbles never touched the fURS tip, and the return for the stone powder was lower than at 2 mm. Keeping the same frequency and the same energy and changing only the pulse length,

we observed that the bubble generated with short pulses was always larger than that generated with long pulses, regardless of the scenario (Fig. 5 Table 3).

## Discussion

The pulses generated by the Ho:YAG laser are capable of cutting the steel wires of a basket, guidewires, and many other materials. The damage to baskets and guidewires induced by the pulses of the Ho:YAG laser are attributed to the high temperatures generated at the tip of the fiber.<sup>7,8</sup> Kang et al. demonstrated that greater heat dissipation with a thicker liquid layer reduces ablation efficiency. This means that the closer the laser tip is to the target, the greater the efficiency, and at the same time, the farther the laser tip is from the fURS scope, the less the damage created.<sup>9</sup> We agree with Cecchetti et al., who wrote that when using the Ho:YAG laser, it is essential that no procedure should be performed without clear and accurate visual control to ensure that the fiber tip is in contact only with the target and sufficiently far from the ureteral wall to avoid the damage that the cavitation bubble can cause to healthy soft tissues. Cecchetti also noted that an adequate distance is necessary from the baskets and guidewires present in the urinary tract to avoid damage.<sup>10</sup>

Canales et al. reviewed the data on fURS repairs of their systems from 2000 to 2004. They had 324 repairs: 30% involved the distal part of the scopes, and 4% were repairs to the objective lens, C-cover, and cover glass.<sup>3</sup> In a retrospective study of the reasons for repairs of four instruments after 655 consecutive ureterorenoscopies in a single center, Kramolowsky et al.<sup>11</sup> reported clouded lens to be the most common damage. Several groups have previously reported either institutional or manufacturer data regarding the causes and location of fURS damage. Sung et al. reported that more than 50% of the damage occurred in the working channel (laser burn in the working channel) or extreme ureteroscope deflection.<sup>12</sup>

Shangguan et al. investigated the effects of density, viscosity, and mechanical strength on laser-induced cavitation bubbles formed in absorbing liquids (e.g., blood, contrast medium, or

saline solution). They found that the bubble dynamics strongly depended on the physical properties of the absorbing liquid and that cavitation bubbles were larger in saline solution than in liquid with a higher density.<sup>13</sup> Therefore, we can assume that, in the presence of liquid with a higher density than saline solution, with the same laser settings, the cavitation bubble generated by the laser machine will be smaller.

The appearance on the screen of the laser fiber at different distances depends on the brand of the scope. Given that fURSs have a 0° camera, it is important to be aware that when the fiber becomes visible on the screen, as our data suggest, it is already at least 1 mm out from the scope. This knowledge is fundamental for avoiding accidental trauma to the urothelial epithelium while manipulating the scope. We observed that in four fURSs over seven, the fiber barely appeared on the screen at a distance of <2 mm. In all scopes, when observed at one-quarter of the screen, the fiber was out 3 mm or more (Fig. 6). Matching these results with the observation that the bubble generated by the Ho-YAG when the laser fiber is at a distance of 3 mm from the fURS tip is never touching the camera of the scope even with high energy and short pulse, we can establish this position as the “safety distance” for avoiding fURS tip damage.

Some difficult cases can oblige the surgeon to use the fiber at the first appearance of the endoscopic screen. In this case, we suggest using low energy ( $\leq 0.5$  J) and long pulse duration because the maximum radius of the bubble is a function of the energy and pulse duration of the laser pulse.<sup>14</sup> If a higher energy is required, we suggest using it for a short time to avoid instrument damage. However, there are few data about camera deterioration. We propose that laser energy hitting the scope using a long distance could damage the fURS tip, including the camera glass and light source. One important limitation of this study was that we could not measure and evaluate damage to the fURS tip surface because several new fURSs would be

needed to complete a full evaluation. Further studies are needed to assess the real damage to the scope tip.

## Conclusion

The aim of this report is to provide some recommendations for using the fiber laser of fURS systems. Based on our findings, we believe that it is safe to position the laser tip at one-quarter of the distance to the monitor because, at this distance with all scopes tested, the Holmium laser energy did not return to the instrument camera. We call this the “safety distance.” In difficult cases, when it may be necessary to have the laser fiber closer to the scope, it is advisable to use the lowest energy possible and a long pulse duration according to the nature of the tissue being treated.

## Acknowledgments

Dr. Esteban Emiliani is sponsored by an European Urological Scholarship Programme (EUSP) scholarship.

## Author Disclosure Statement

No competing financial interests exist.

## References

1. Somani BK, Robertson A, Kata SG. Decreasing the cost of flexible ureterorenoscopic procedures. *Urology* 2011;78:528–530.
2. Chapman RA, Somani BK, Robertson A, et al. Decreasing cost of flexible ureterorenoscopy: Single-use laser fiber cost analysis. *Urology* 2014;83:1003–1005.
3. Canales BK, Gleason JM, Hicks N, et al. Independent analysis of Olympus flexible ureteroscope repairs. *Urology* 2007;70:11–15.

4. Pietrow PK, Auge BK, Delvecchio FC, et al. Techniques to maximize flexible ureteroscope longevity. *Urology* 2002;60:784–788.
5. User HM, Hua V, Blunt LW, et al. Performance and durability of leading flexible ureteroscopes. *J Endourol* 2004;18:735–738.
6. Esch E, Simmons WN, Sankin G, et al. A simple method for fabricating artificial kidney stones of different physical properties. *Urol Res* 2010;38:315–319.
7. Tasca A, Cecchetti W. Laser—Lasertrissia dei calculi in urologia. *Enciclopedia Medica Italiana* 1999; 11:3102–3108.
8. Freiha GS, Glickman RD, Teichman MH. Holmium:YAG laser-induced damage to guide wires: experimental study. *J Endourol* 1997;11:331–336.
9. Kang HW, Welch AJ. Effect of liquid thickness on laser ablation efficiency. *J Appl Phys* 2007;101:083101.
10. Cecchetti W, Zattoni F, Nigro F, et al. Plasma bubble formation induced by holmium laser: an in vitro study. *Urology* 2004;63:586–590.
11. Kramolowsky E, Booth B, McDowell Z, et al. Cost analysis of flexible ureteroscope repairs: evaluation of 655 procedures in a community-based practice. *J Endourol* 2016;30:254–256.
12. Sung JC, Springhart P, Marguet CG, et al. Location and etiology of flexible and semirigid ureteroscope damage. *Urology* 2005;66:958–963.
13. Shangguan H, Casperson LW, Shearin A, et al. Effects of material properties on laser induced bubble formation in absorbing liquids and on submerged targets. In: *Diagnostic and Therapeutic Cardiovascular Interventions VII*, D. L. Paisley and A. M Frank Eds., *Proc. SPIE* 1997;2869:783–791.

14. Jansen ED, Asshauer T, Frenz M, et al. Effect of pulse duration on bubble formation and laser-induced pressure waves during holmium laser ablation. *Lasers Surg Med* 1996;18:278–293.

#### ABBREVIATION USED

flexible ureterorenoscopes = fURSSs

frames per second = fps

fiber-optic flexible ureterorenoscopes = OU

digital flexible ureterorenoscopes = DU

Holmium laser YAG = Ho:YAG



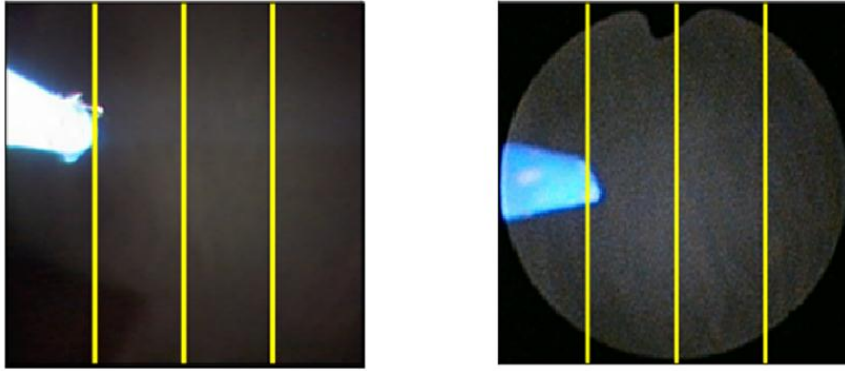


**FIG. 1.** Laser fiber at one-quarter of the screen in a digital (A) and an optical (B) fURS.

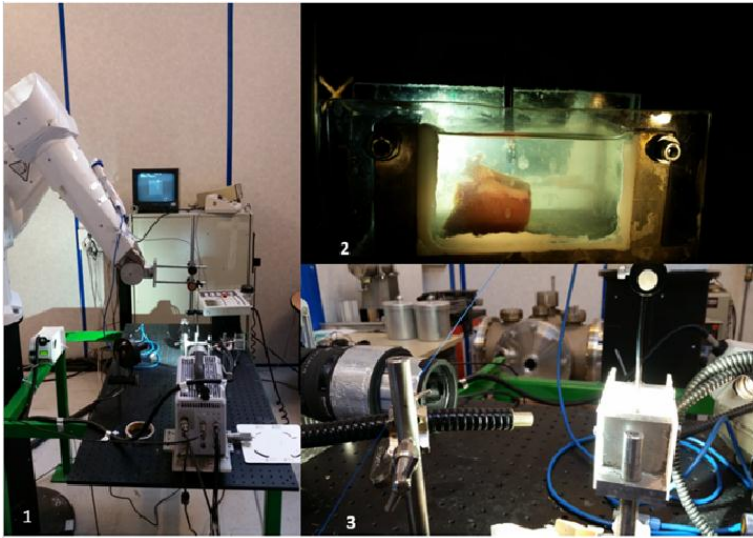


**FIG. 2.** Lab setting: 2-1 working table with the fURS hanging on the robotic arm on the left side and the high-speed camera in the center of the table; 2-2 bowl with a sample of pork kidney and the fURS coming from the top; 2-3 the table setting.

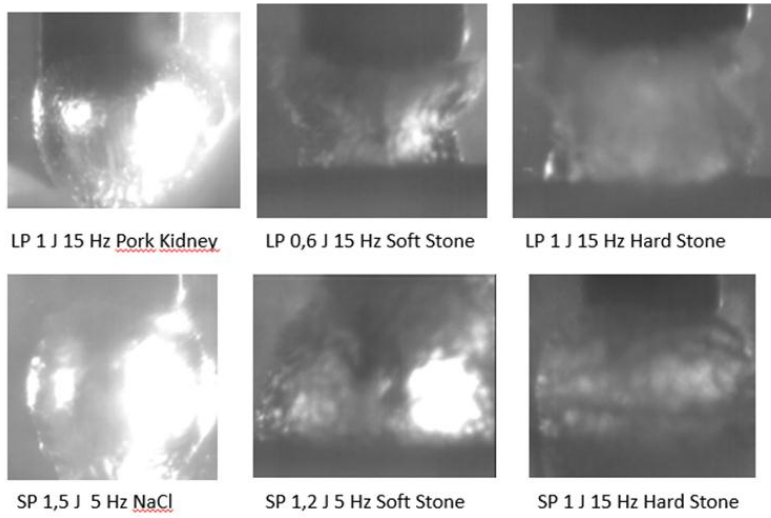


**FIG. 3.** Different laser bubbles touching the scope at a distance of 1 mm.

LP = long pulse; SP = short pulse

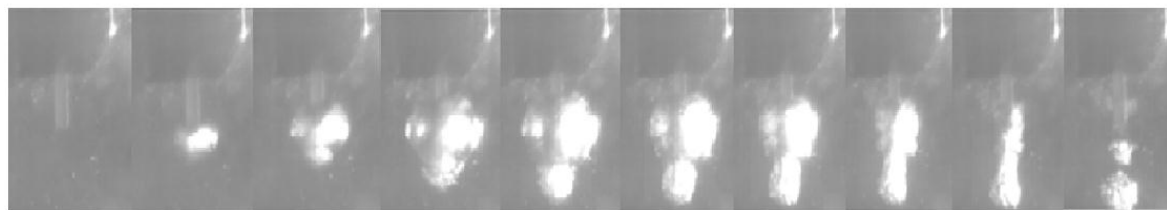


**FIG. 4.** Bubble created by the 273  $\mu\text{m}$  laser fiber at a distance of 1 mm from the scope in 0.9% NaCl with energy of 0.5 J, frequency of 15 Hz, and long pulse duration. The bubble does not touch the tip of the fURS.

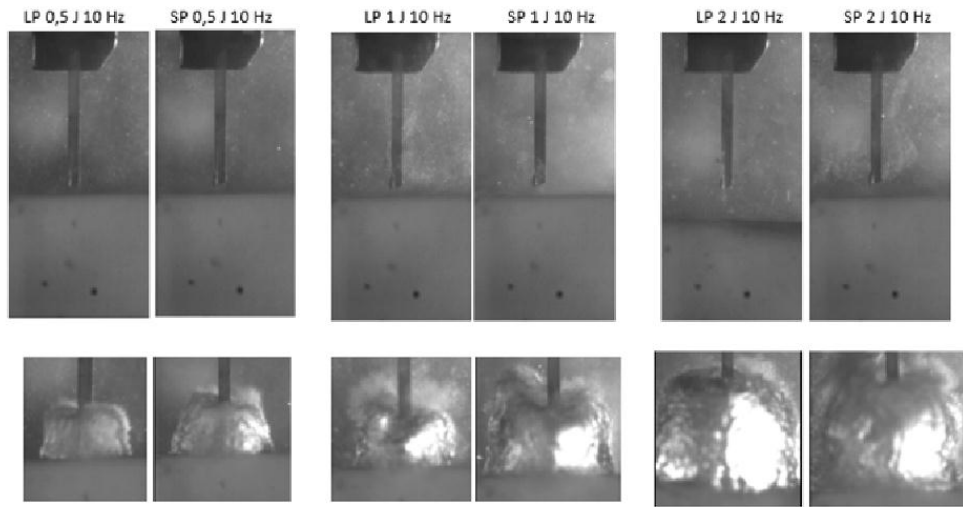


**FIG. 5.** Comparison of bubbles generated at the same energy with different pulse lengths in 0.9% NaCl without any surface in front and with a soft synthetic BegoStone. The laser fiber is 3 mm outside the scope.

LP = long pulse; SP = short pulse.

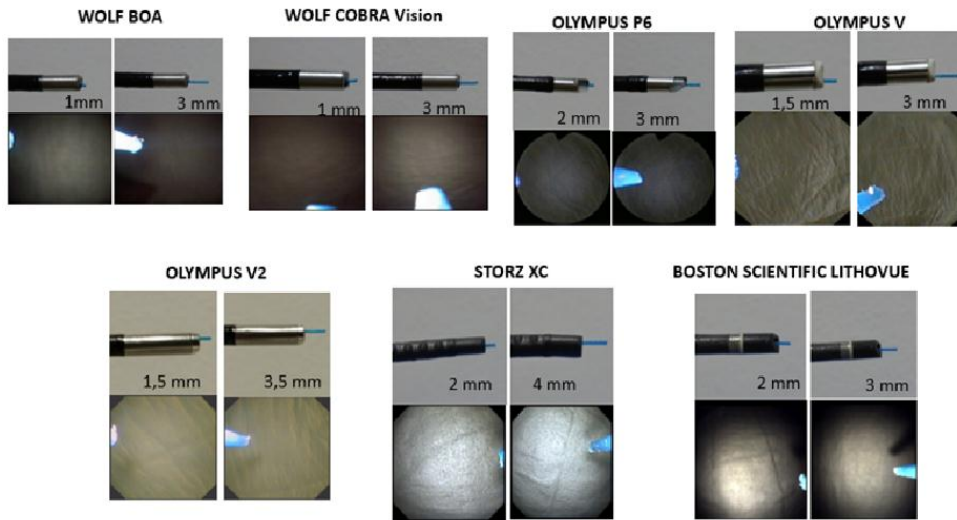


**FIG. 6.** Images of the fiber distance at D1 and D2 in different fURSSs: external view and endo view.

TABLE 1. D1 FIRST APPEARANCE OF THE LASER FIBER ON THE SCREEN; D2 LASER FIBER DISTANCE AT ONE-QUARTER OF THE SCREEN

<i>Instrument</i>	<i>D1 (mm)</i>	<i>D2 (mm)</i>
Olympus P6	2	3
Olympus V	1.5	3
Olympus V2	1.5	3.5
Wolf Boa	1	3.3
Wolf Cobra Vision	1	3
Storz XC	2	4
LithoVue	2	3

TABLE 2. PRESETTING SUGGESTED BY THE MACHINE TO SIMULATE FRAGMENTATION AND DUSTING WITH STONE PHANTOMS AND RESECTION WITH PORK KIDNEY

<i>Material</i>	<i>Setting for dusting</i>	<i>Setting for fragmentation</i>
Nothing	LP 0.5 J, 15 Hz	SP 1.5 J, 5 Hz
Hard stone	LP 1.0 J, 15 Hz	SP 1.5 J, 5 Hz
Soft stone	LP 0.6 J, 15 Hz	SP 1.2 J, 5 Hz
Pork kidney	LP 1.0 J, 15 Hz	

J = Joule; Hz = Hertz; LP = long pulse; SP, short pulse. The settings were recorded at a distance of the laser fiber of 1, 2, or 3 mm.



TABLE 3. THE TWO LARGER BUBBLE DIAMETERS COMPARED BETWEEN LONG AND SHORT PULSES AT THE SAME ENERGY LEVEL

<i>Condition</i>	<i>Long pulse</i>		<i>Short pulse</i>	
	<i>Horizontal diameter (mm)</i>	<i>Vertical diameter (mm)</i>	<i>Horizontal diameter (mm)</i>	<i>Vertical diameter (mm)</i>
0.9% NaCl				
0.5 J, 10 Hz	2.400	2.438	2.775	2.850
1.0 J, 10 Hz	3.301	3.637	3.301	3.750
2.0 J, 10 Hz	3.600	4.613	4.807	4.877
Soft stone				
0.5 J, 10 Hz	2.444	1.519	2.704	1.852
1.0 J, 10 Hz	2.852	2.111	3.370	2.817
2.0 J, 10 Hz	3.889	3.412	4.259	3.666

The bubble generated with short pulses was always larger than that generated with long pulses. The two major diameters were measured using ImageJ software.